BOLETIN DE LA SOCIEDAD ESPAÑOLA DE
Cerámica y Vidrio
www.elsevier.es/bsecv

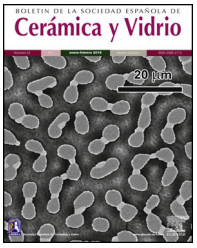

Two-step liquid-phase synthesis of argyrodite Li_6PS_5Cl solid electrolyte using nonionic surfactant

Nataly Carolina Rosero-Navarro[a,*], *Hazuki Niwa*[b], *Akira Miura*[a], *Kiyoharu Tadanaga*[a]

[a] *Division of Applied Chemistry, Faculty of Engineering, Hokkaido University, Sapporo 060-8628, Japan*
[b] *Graduate School of Chemical Sciences and Engineering, Hokkaido University, Sapporo 060-8628, Japan*

ARTICLE INFO

Article history:
Received 11 August 2021
Accepted 3 December 2021
Available online 20 December 2021

Keywords:
Sulfide solid electrolyte
Liquid-phase synthesis
Particle size control
High ionic conductivity

ABSTRACT

In the present work, argyrodite Li_6PS_5Cl sulfide solid electrolyte is prepared by a liquid phase process, consisting of two steps: (1) suspension-reaction under the ultrasonication of Li_2S, P_2S_5, and LiCl precursors in acetonitrile and, (2) dissolution-precipitation involving the addition of ethanol/acetonitrile and solvents removal by heating at 180 °C. The effect of the addition of a nonionic surfactant on the properties of the sulfide solid electrolyte is also studied. The synthesis process allows to obtain Li_6PS_5Cl argyrodite solid electrolyte with high ionic conductivity of 2.0×10^{-4} S cm^{-1}, the low activation energy of 0.22 eV, and electrochemical stability up to 5 V (vs. Li). A regular particle distribution with a size smaller than 1 μm is obtained by the addition of the surfactant.

Síntesis en fase líquida en 2 pasos del electrolito sólido de argirodita Li_6PS_5Cl utilizando un surfactante no iónico

Palabras clave:
Electrolito sólido de sulfuro
Síntesis en fase líquida
Control del tamaño de partículas
Alta conductividad iónica

RESUMEN

En el presente trabajo, el electrolito sólido de sulfuro argirodita Li_6PS_5Cl se prepara mediante un proceso en fase líquida, que consta de 2 pasos: 1) suspensión-reacción bajo radiación ultrasónica de los precursores de Li_2S, P_2S_5 y LiCl en acetonitrilo, y 2) disolución-precipitación que involucra la adición de etanol/acetonitrilo y eliminación de disolventes a 180 °C. También se estudia el efecto de la adición de un surfactante no iónico sobre las propiedades del electrolito sólido de sulfuro. El proceso de síntesis permite obtener electrolito sólido Li_6PS_5Cl con alta conductividad iónica de $2{,}0 \times 10^{-4}$ S cm^{-1}, baja energía

* *Corresponding author.*
E-mail address: rosero@eng.hokudai.ac.jp (N.C. Rosero-Navarro).
https://doi.org/10.1016/j.bsecv.2021.12.001

de activación de 0,22 eV y estabilidad electroquímica de hasta 5 V (vs. Li). Se obtiene una distribución regular de partículas con un tamaño inferior a 1 μm mediante la adición del surfactante.

Introduction

All-solid-state batteries based on sulfide solid electrolytes are actively investigated because sulfide solid electrolytes have high ionic conductivity (10^{-2}–10^{-4} S cm^{-1}) and form low interfacial electrode–electrolyte resistance by simple cold pressure procedure [1,2]. The sulfide solid electrolytes have been commonly prepared by mechanical milling and high-temperature solid-state synthesis [2]. Recently, the liquid phase syntheses [3,4] have attracted much attention as a versatile chemical route to prepare sulfide solid electrolytes since this is considered more practical from a mass-produce point of view through reducing processing time and thermal treatments.

According to the literatures [3–5], there are so far two differentiated routes to prepare sulfide solid electrolyte by liquid-phase synthesis: (i) dissolution-precipitation of sulfide solid electrolyte precursor, previously obtained by mechanical milling or solid-state reactions [6–16] and, (ii) suspension-reaction of the precursors without any previous mechanochemical reaction [17–27]. Solvents such as hydrazine, N-methylformamide, and ethanol are used to dissolve the sulfide electrolytes. In the suspension-reaction process, the precursors (Li_2S, P_2S_5, LiI, etc.), without previous reaction, are dispersed into a solvent such as acetonitrile, tetrahydrofuran or 1,2-dimethoxyethane. The reactions are promoted by the stirring process or accelerated by shaking [21,25] (using zirconia balls) or ultrasonic irradiation [24,26] processes. In both cases, the solvents are removed at temperatures above 100 °C. A combined approach (two-step liquid-phase synthesis) using suspension-reaction and dissolution-precipitation has also been explored to prepare sulfide solid electrolytes [28–30].

From the point of view of the application in all-solid-state batteries, a liquid-phase synthesis that involves the dissolution of the sulfide electrolyte is more advantaged. For instance, the precipitation of the sulfide electrolyte, crucial for compaction of the material, could be controlled by selecting the solvents, evaporation rate, or the use of surfactants. Furthermore, the use of a precursor solution of sulfide solid electrolyte is also especially favorable for the preparation of composite electrodes since it can effectively cover the solids particles of active material, improving the percolation of the sulfide solid electrolyte (lithium pathway) through them. Therefore, a low interfacial electrode–electrolyte resistance is fabricated.

Among sulfide electrolytes, argyrodite-type Li_6PS_5X (X = Cl, Br) solid electrolytes are attractive materials formed by PS_4^{3-}, S^{2-}, X^- and Li^+ ions [29,31]. Their preparation by two-step liquid-phase synthesis has been reported [28–30], following the next reactions:

$$3Li_2S + P_2S_5 \rightarrow 2Li_3PS_4 \quad (1)$$

suspension-reaction using tetrahydrofuran (THF) or ethyl propionate (EP)

$$Li_3PS_4 + Li_2S + LiX \rightarrow Li_6PS_5X \quad (2)$$

dissolution-precipitation using ethanol

The ionic conductivity of the argyrodite electrolytes by this two-step liquid phase process varies in almost one order of magnitude depending on the solvent medium, achieving 1.3×10^{-4} and 3.4×10^{-5} S cm^{-1} for the THF-ethanol and EP-ethanol system, respectively [28,29]. In the present work, argyrodite Li_6PS_5Cl sulfide solid electrolyte is prepared by a two-step liquid phase process using a different solvent medium, acetonitrile for suspension-reaction and ethanol/acetonitrile for dissolution-precipitation, respectively. The effect of nonionic surfactant on the properties of the argyrodite electrolyte is also studied. A nonionic surfactant such as Triton X-100 ($C_{14}H_{22}O(C_2H_4O)_8$, t-octylphenoxypolyethoxy-ethanol) is expected to be less reactive to the sulfide electrolyte precursor and prevent side reactions while the morphology can be controlled.

Experimental

The solid electrolytes were prepared in a glove box under an argon atmosphere. The characterizations were also carried out under an inert atmosphere using adequate transfer holders to prevent undesired reactions with moisture.

Fig. 1a illustrates the synthesis procedure of Li_6PS_5Cl solid electrolyte by liquid phase process using a suspension-reaction process followed by a dissolution-precipitation process. Typically, 0.5 g of stoichiometric proportions of Li_2S (Mitsuwa's Purity Chemicals, 99.9%), P_2S_5 (Sigma–Aldrich, 99%), and LiCl (Sigma–Aldrich, 99.9%) were mixed in an agate mortar for 5 minutes. The mixed powder was transferred to a glass vessel with 10 mL of acetonitrile (99.5%, Wako Pure Chemical, Japan). The mixture was ultrasonicated for 60 min at 60 °C under 45 kHz using an ultrasonic bath (Shimadzu SUS-103). The reaction was verified by the formation of a white suspension. Then, 15 mL ethanol (99.5%, Wako Pure Chemical, Japan) and 15 mL acetonitrile were added to obtain a yellowish transparent solution (Fig. 1a). Note that ethanol is mostly used to dissolve the sulfide electrolyte while acetonitrile can partially contribute to the dissolution [32]. The effect of the surfactant was studied through the addition of 0.1 wt% of Triton X-100 to Li_6PS_5Cl-solution. Triton X-100 is a nonionic surfactant which has a hydrophilic polyethylene oxide chain and an aromatic hydrophobic group. The solid electrolyte solution was dried at and 180 °C for 4 h under vacuum to remove the solvent and obtain solid powders.

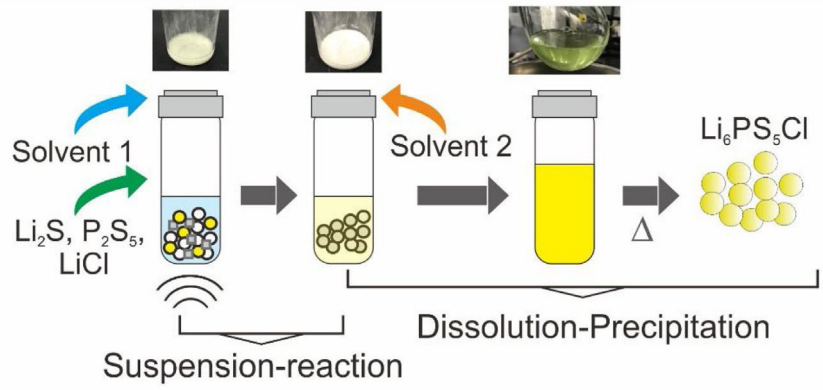

Fig. 1 – Illustration of synthesis of Li_6PS_5Cl by two-step liquid phase process. Solvent 1: acetonitrile, Solvent 2: ethanol/acetonitrile.

Crystal phase, morphology, and electrochemical properties of the Li_6PS_5Cl solid electrolyte were examined to elucidate the effect of the solvent medium including the surfactant on the properties of the sulfide solid electrolyte obtained by the two-step liquid phase process. Crystal phase evaluated by X-ray diffraction (XRD) was carried out with an X-ray diffractometer (MultiFlex600, Rigaku) using CuKα radiation (1.5418 Å) in the 2θ scan range of 20–40°. XRD analysis by SmartLab Studio II software. Morphology was observed by scanning electron microscopy (SEM), performed on a JIB-4600F Multibeam SEM-FIB Scanning Electron Microscope. Electrochemical properties of Li_6PS_5Cl solid electrolyte were evaluated by electrochemical impedance spectroscopy (EIS) and cyclic voltammetry (CV) techniques. EIS was carried out using impedance analyzer (SI 1260, Solartron) in a frequency range of 1 and 1×10^6 Hz at temperatures between 22 °C and 84 °C. The solid electrolyte powder (80 mg) was pressed under 360 MPa (at room temperature) in a polycarbonate tube 10 mm in diameter. Two stainless steel (SS) disks were used as current collectors. The ohmic total resistance (Rt) was normalized to the pellet geometry, thickness (t) and surface area (A), to calculate the conductivity through the formula $\sigma = t/Rt \cdot A$. The geometric density of pellets was calculated from the weight and geometric dimensions. For the CV measurements, a potentiostat/galvanostat device (SI 1287, Solartron) was used in the potential range of −0.5 V to 5 V (vs. Li/Li+) at a scanning rate of 1 mV s^{-1}. Li–In alloy foil was attached to one of the pellet faces and two SS disks were used as current collectors.

Results and discussion

Fig. 2a shows the X-ray diffraction (XRD) patterns of powder samples obtained by the two-step liquid phase process without and with 0.1 wt% surfactant. The indexed XRD pattern of the $Li_{6.2}PS_5Cl$ (ICDD #418490) phase was included for comparison.

The argyrodite phase was obtained after the two-step liquid phase process, verifying that a short reaction time of 60 min (under ultrasonication) is enough to promote the reaction of Li_2S, P_2S_5, (Li_3PS_4) and LiCl precursors [28]. The small peaks centered at ~27° and ~35° corresponding to Li_2S and

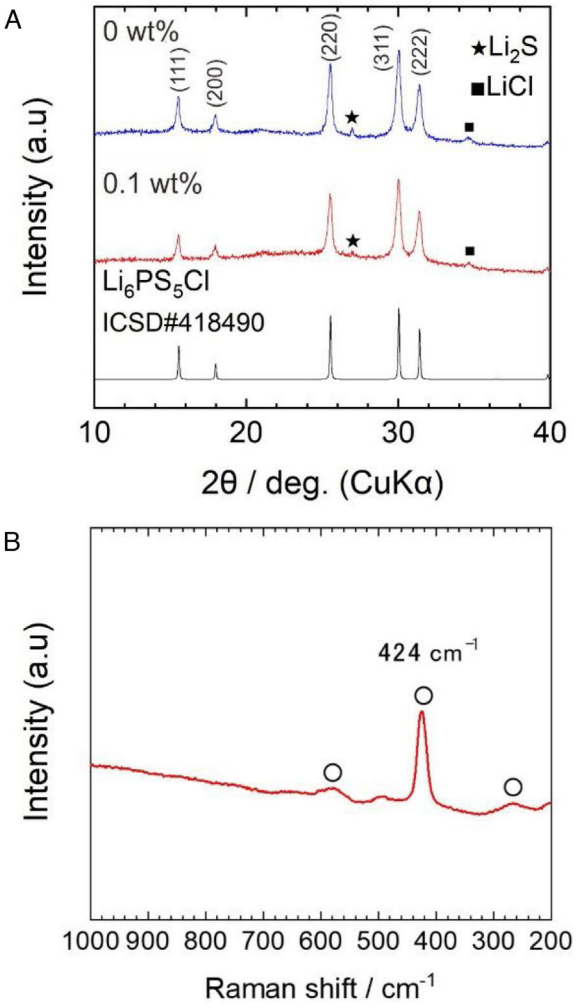

Fig. 2 – (a) XRD patterns of Li_6PS_5Cl obtained by two-step liquid phase process without and with 0.1 wt% surfactant. XRD pattern of Li_6PS_5Cl phase (ICDD#418490) is included. (b) Raman spectra of the Li_6PS_5Cl sulfide electrolyte (0.1 wt% surfactant).

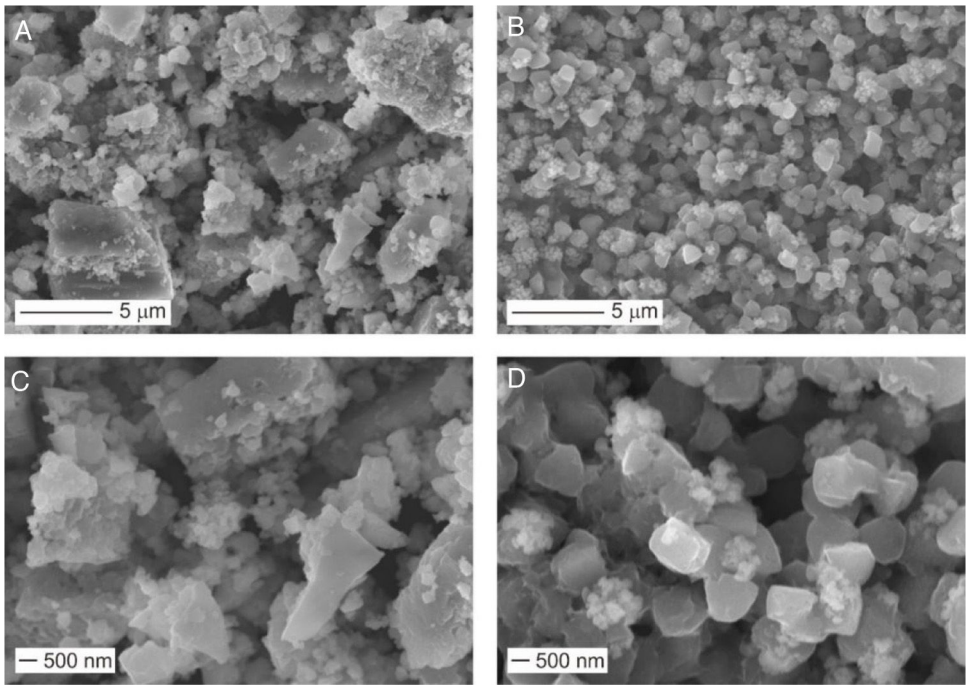

Fig. 3 – SEM images of Li_6PS_5Cl obtained by two-step liquid phase process: (a) and (c) without surfactant and, (b) and (d) with 0.1 wt% surfactant.

LiCl were also observed. The XRD powder patterns were indexed as a cubic cell with lattice parameters of 9.856(9) and 9.853(2) Å for the solid electrolyte obtained by the liquid phase process without and with 0.1 wt% surfactant, respectively. Lattice parameters coincide with those given in the literature (ICSD#418490: 9.850(4) Å). The slightly larger lattice is related to the plausible formation of sub-stoichiometry chlorine phases ($Li_{7-x}PS_{6-x}Cl_x$) [33]. The presence of the surfactant does not show significant changes in the XRD patterns. On the other hand, the full width at half maximum (FWHM) values of Li_6PS_5Cl with surfactant were larger than Li_6PS_5Cl without surfactant. For reference, from the intense peak on plane (220) at 2θ of 25.5°, FMHW is 0.279° and 0.2944° for Li_6PS_5Cl without and with 0.1 wt% surfactant, respectively. This suggests that the average crystallite size [34] should be smaller in the case of Li_6PS_5Cl with 0.1 wt% surfactant.

Fig. 2b displays a Raman spectrum of Li_6PS_5Cl solid electrolyte obtained by liquid phase process with 0.1 wt% surfactant. Bands located at 266 cm^{-1}, 424 cm^{-1}, and 580 cm^{-1} are associated with PS_4^{3-} units, which are structural units of argyrodite structure. Moreover, the absence of bands associated with the solvents or surfactant, such as vibrational mode of skeletal C—C—O stretching at ~884 cm^{-1} from ethanol [9] or vibrational mode of C—C≡N bending at ~370 cm^{-1} from acetonitrile [24], verified their major removal after heat treatment at low temperatures of 180 °C and negligible effect of the addition of the surfactant on the argyrodite structure.

Fig. 3 shows the morphology of the Li_6PS_5Cl solid electrolyte obtained by liquid phase process without and with 0.1 wt% surfactant.

Irregular particles with different sizes were observed in the Li_6PS_5Cl solid electrolyte powder derived from the solution without the surfactant. The particle size varies from big particles or agglomerates up to 2–5 μm (Fig. 3a) and small particle sizes of lower than 500 nm (Fig. 3c). The small particles (<500 nm) were also observed in the Li_6PS_5Cl solid electrolyte powder derived from the solution containing the surfactant (Fig. 3d). However, big particles or agglomerates were not observed (Fig. 3b). Contrarily, particles with regular distribution with *quasi* spherical shape and small particle size lower than 1 μm were observed (Fig. 3d). Particles with regular and small size in the nanometric scale have been observed in the sulfide solid electrolytes such as $Li_7P_3S_{11}$ and β-Li_3PS_4 derived from a liquid phase process, especially using aprotic solvents such acetonitrile or tetrahydrofuran [26,35,36]. The solvent is also believed to play a surfactant role in the growth of sulfide solid electrolyte particles [35], allowing more particles to escape the aggregation process by modification of their interfacial surface tension and resulting in small particles sizes. The mechanism of the precipitation of sulfide solid electrolyte by a liquid phase process involves the formation of intermedium complexes between particles and solvent during the process is known [26,32,36–38]. These complexes may be responsible for changing the surface tension of the particles. The effect is remarkable in the addition of the surfactant, where the surface tension created between the particles and surrounding organic medium (acetonitrile, ethanol, and surfactant) leads to the precipitation of particles with a regular size and shape (Fig. 3b and d).

Fig. 4a shows AC impedance plots of Li_6PS_5Cl solid electrolyte obtained by the liquid phase process without and with 0.1 wt% surfactant. The Nyquist plots of Li_6PS_5Cl solid electrolyte without the surfactant consist in an incomplete resolved semicircle at high frequency (0.7 MHz) and a

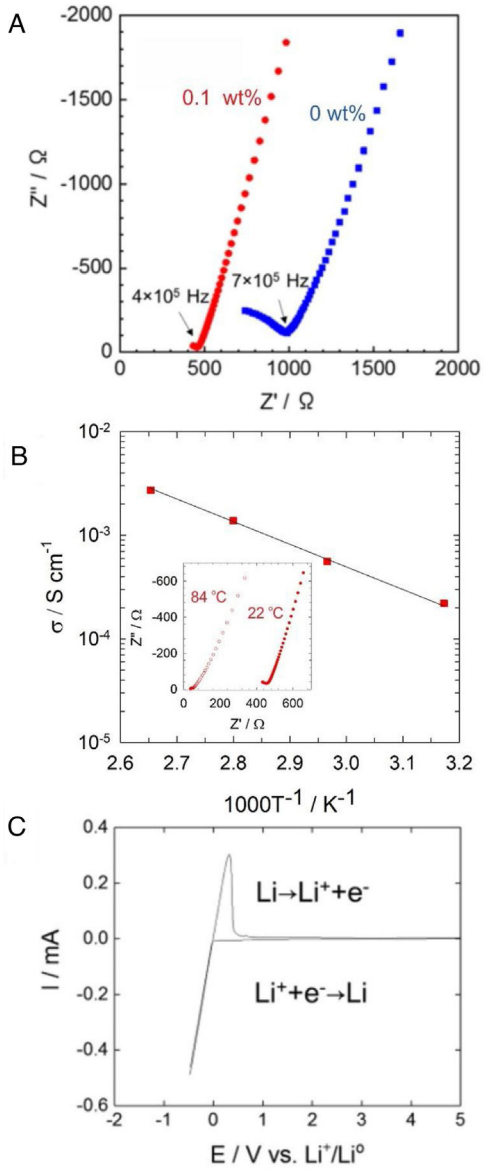

Fig. 4 – (a) Impedance profile of the pelletized Li_6PS_5Cl obtained by two-step liquid phase process without and with 0.1 wt% surfactant at 22 °C. (b) Temperature dependency of the ionic conductivity of Li_6PS_5Cl (0.1 wt% surfactant). Inset shows impedance profile for 22 °C and 84 °C. (c) Cyclic voltammogram of Li_6PS_5Cl (0.1 wt% surfactant).

capacitive tail at low frequency due to the interface between the ionic conductor and blocking stainless steel electrodes. The lower resistance of the Li_6PS_5Cl solid electrolyte with 0.1 wt% surfactant results in a capacity tail with very few points at higher frequencies (0.4 MHz). Both impedance spectra were fitted with a linear fit of a capacitive tail to assess the resistance value of Z′ at the intercept with the real axis. This total resistance consists of grain and grain boundary contributions and achieves 986.2 Ω and 464.2 Ω for Li_6PS_5Cl without and with 0.1 wt% surfactant, respectively. The ionic conductivity of the Li_6PS_5Cl attains 0.9×10^{-4} S cm^{-1} ($\rho = 1.43$ g cm^{-3}) and 2×10^{-4} S cm^{-1} ($\rho = 1.43$ g cm^{-3}) at room temperature for the samples derived from the Li_6PS_5Cl solution without and with 0.1 wt% surfactant, respectively. The difference of ionic conductivity of Li_6PS_5Cl derived from solution without and with the surfactant must be attributed to the different morphology of each powder observed by SEM as described above (Fig. 3). Although the density does not change significantly, the regular distribution of particle size may produce better densification and lithium-ions percolation (i.e., less porous or void microstructure) by cold-press procedure and therefore a better ionic conductivity.

Fig. 4b shows the temperature dependence of the ionic conductivity of the Li_6PS_5Cl derived from the solution with 0.1 wt% surfactant between 22 °C and 84 °C. The activation energy of 0.22 eV was obtained using the slope of the curve. Fig. 4c shows the cyclic voltammogram of the Li_6PS_5Cl derived from the solution with 0.1 wt% surfactant, from −0.5 V to 5 V (vs. Li/Li$^+$). The lithium deposition ($Li^+ + e^- \rightarrow Li$) and dissolution ($Li \rightarrow Li^+ + e^-$) reactions were observed in the potential range of −0.5 V to 0.5 V, corresponding to cathodic and anodic current peaks. The absence of any electrochemical response in the range of the potential up to 5 V suggests high electrochemical stability of Li_6PS_5Cl obtained by the two-step liquid phase process.

The ionic conductivity of Li_6PS_5Cl prepared by ball-milling process depends on parameters such as time of milling (5–50 h) and further heat treatment (cooling-heating) up to ca. 550 °C [31,33,39–43]. In general terms, high-crystallized sample achieves 10^{-3} S cm^{-1} and low activation energy of around 0.16 eV, while low-crystallized sample displays lower ionic conductivity (10^{-4}–10^{-5} S cm^{-1}) and higher activation energy around 0.3–0.4 eV [31,33,39–43]. Rao et al. [33] have studied the mechanism of formation of argyrodite Li_6PS_5Cl phase by ball milling and subsequent heat-cooling treatment. Their studies of heat-cooling treatment suggest the formation of Li_7PS_6 phase during the first stage of the argyrodite phase, where temperatures: ca. 190 °C are needed to incorporate Cl in the structure ($Li_{7-x}PS_{6-x}Cl_x$), ca. 250 °C are required to obtain the stoichiometric Li_6PS_5Cl phase, and >250 °C are used to increase the crystallinity of Li_6PS_5Cl phase. Thus, the substoichiometric $Li_{7-x}PS_{6-x}Cl_x$ phases show conductivities around 10^{-4} S cm^{-1}, while the stoichiometric Li_6PS_5Cl phase attains high ionic conductivity of 1×10^{-3} S cm^{-1} and a low activation energy of 0.16 eV [33]. In the present study, Li_6PS_5Cl solid electrolyte obtained by the two-step liquid phase process shows an ionic conductivity of 2×10^{-4} S cm^{-1} with a low activation energy of 0.22 eV. The results suggest that ionic conductivity is governed mostly by the crystallinity of the sample, however, the partial formation of substoichiometric $Li_{7-x}PS_{6-x}Cl_x$ phases (verified by the small peaks of Li_2S and LiCl in XRD patterns, Fig. 2a) could be responsible for the slight reduction in the expected ionic conductivity.

Compared with analogous argyrodite-type electrolytes prepared by similar liquid-phase synthesis [28–30], the current argyrodite electrolyte shows a slight enhancement of the ionic conductivity attributed to the regular particle size obtained by using the surfactant. Modifications in the argyrodite electrolyte including their composition or use of additives, easily performed by the liquid-phase synthesis, are believed to be a key to the further enhancement of the ionic conductivity of argyrodite-type electrolytes.

Conclusion

The two-step liquid phase process is a potential technique to prepare sulfide solid electrolytes with high ionic conductivity. Li_6PS_5Cl solid electrolyte was prepared by a two-step liquid phase process, combining suspension-reaction and dissolution-precipitation processes. Ultrasonic irradiation of Li_2S, P_2S_5, and LiCl precursors using acetonitrile as a solvent for 1 h promoted the reaction. The dissolution and subsequent thermal treatment at 180 °C lead to the precipitation of the argyrodite crystal phase, and the addition of the surfactant allowed to control of the morphology of Li_6PS_5Cl particles. As a result, the solid electrolyte achieved a high ionic conductivity of 2.0×10^{-4} S cm^{-1} with a low activation energy of 0.22 eV and electrochemical stability up to 5 V (vs. Li).

Conflict of interest

The authors declare no conflict of interest.

Acknowledgements

The present work was supported by the Japan Science and Technology Agency (JST), Advanced Low Carbon Technology Research and Development Program, and Specially Promoted Research for Innovative Next Generation Batteries (ALCA-SPRING) project. This research was partially supported by KAKENHI Grants JP21H01610. The analysis of SEM was carried out with JIB-4600F at the "Joint-use Facilities: Laboratory of Nano-Micro Material Analysis", Hokkaido University, supported by "Material Analysis and Structure Analysis Open Unit (MASAOU)".

REFERENCES

[1] G. Bucci, T. Swamy, Y.M. Chiang, W.C. Carter, Modeling of internal mechanical failure of all-solid state batteries during electrochemical cycling, and implications for battery design, J. Mater. Chem. A 5 (2017) 19422–19430.
[2] A. Hayashi, A. Sakuda, M. Tatsumisago, Development of sulfide solid electrolytes and interface formation processes for bulk-type all-solid-state Li and Na batteries, Front. Energy Res. 4 (2016).
[3] K.H. Park, Q. Bai, D.H. Kim, D.Y. Oh, Y. Zhu, Y. Mo, Y.S. Jung, Design strategies practical considerations, and new solution processes of sulfide solid electrolytes for all-solid-state batteries, Adv. Energy Mater. 8 (2018) 1800035.
[4] A. Miura, N.C. Rosero-Navarro, K. Tadanaga, N.H.H. Phuc, A. Matsuda, N. Machida, A. Sakuda, A. Hayashi, M. Tatsumisago, Liquid-phase chemistry of sulfide electrolytes for all-solid-state lithium battery, Nat. Rev. Chem. 3 (2019) 189–198.
[5] K. Tadanaga, N.C. Rosero-Navarro, A. Miura, Wet chemical processes for the preparation of composite electrodes in all-solid-state lithium battery, in: K. Kanamura (Ed.), Next Generation Batteries: Realization of High Energy Density Rechargeable Batteries, Springer Singapore, Singapore, 2021, pp. 85–92.
[6] S. Teragawa, K. Aso, K. Tadanaga, A. Hayashi, M. Tatsumisago, Formation of Li_2S-P_2S_5 solid electrolyte from N-methylformamide solution, Chem. Lett. 42 (2013) 1435–1437.
[7] Y.M. Wang, Z.Q. Liu, X.L. Zhu, Y.F. Tang, F.Q. Huang, Highly lithium-ion conductive thio-LISICON thin film processed by low-temperature solution method, J. Power Sources 224 (2013) 225–229.
[8] S. Teragawa, K. Aso, K. Tadanaga, A. Hayashi, M. Tatsumisago, Preparation of Li_2S-P_2S_5 solid electrolyte from N-methylformamide solution and application for all-solid-state lithium battery, J. Power Sources 248 (2014) 939–942.
[9] S. Yubuchi, S. Teragawa, K. Aso, K. Tadanaga, A. Hayashi, M. Tatsumisago, Preparation of high lithium-ion conducting Li_6PS_5Cl solid electrolyte from ethanol solution for all-solid-state lithium batteries, J. Power Sources 293 (2015) 941–945.
[10] K.H. Park, D.Y. Oh, Y.E. Choi, Y.J. Nam, L.L. Han, J.Y. Kim, H.L. Xin, F. Lin, S.M. Oh, Y.S. Jung, Solution-processable glass LiI-Li_4SnS_4 superionic conductors for all-solid-state Li-ion batteries, Adv. Mater. (Weinheim, Ger.) 28 (2016) 1874–1883.
[11] Y.E. Choi, K.H. Park, D.H. Kim, D.Y. Oh, H.R. Kwak, Y.G. Lee, Y.S. Jung, Coatable Li_4SnS_4 solid electrolytes prepared from aqueous solutions for all-solid-state lithium-ion batteries, Chemsuschem 10 (2017) 2605–2611.
[12] N.C. Rosero-Navarro, T. Kinoshita, A. Miura, M. Higuchi, K. Tadanaga, Effect of the binder content on the electrochemical performance of composite cathode using Li_6PS_5Cl precursor solution in an all-solid-state lithium battery, Ionics 23 (2017) 1619–1624.
[13] D.H. Kim, D.Y. Oh, K.H. Park, Y.E. Choi, Y.J. Nam, H.A. Lee, S.-M. Lee, Y.S. Jung, Infiltration of solution-processable solid electrolytes into conventional Li-ion-battery electrodes for all-solid-state Li-ion batteries, Nano Lett. 17 (2017) 3013–3020.
[14] S. Yubuchi, M. Uematsu, M. Deguchi, A. Hayashi, M. Tatsumisago, Lithium-ion-conducting argyrodite-type Li_6PS_5X (X = Cl, Br I) solid electrolytes prepared by a liquid-phase technique using ethanol as a solvent, ACS Appl. Energy Mater. 1 (2018) 3622–3629.
[15] N.C. Rosero-Navarro, A. Miura, K. Tadanaga, Composite cathode prepared by argyrodite precursor solution assisted by dispersant agents for bulk-type all-solid-state batteries, J. Power Sources 396 (2018) 33–40.
[16] N.C. Rosero-Navarro, A. Miura, K. Tadanaga, Preparation of lithium ion conductive Li_6PS_5Cl solid electrolyte from solution for the fabrication of composite cathode of all-solid-state lithium battery, J. Sol-Gel Sci. Technol. 89 (2019) 303–309.
[17] Z.C. Liu, W.J. Fu, E.A. Payzant, X. Yu, Z.L. Wu, N.J. Dudney, J. Kiggans, K.L. Hong, A.J. Rondinone, C.D. Liang, Anomalous high ionic conductivity of nanoporous beta-Li_3PS_4, J. Am. Chem. Soc. 135 (2013) 975–978.
[18] S. Ito, M. Nakakita, Y. Aihara, T. Uehara, N. Machida, A synthesis of crystalline $Li_7P_3S_{11}$ solid electrolyte from 1,2-dimethoxyethane solvent, J. Power Sources 271 (2014) 342–345.
[19] E. Rangasamy, Z.C. Liu, M. Gobet, K. Pilar, G. Sahu, W. Zhou, H. Wu, S. Greenbaum, C.D. Liang, An iodide-based $Li_7P_2S_8I$ superionic conductor, J. Am. Chem. Soc. 137 (2015) 1384–1387.
[20] R.C. Xu, X.H. Xia, Z.J. Yao, X.L. Wang, C.D. Gu, J.P. Tu, Preparation of $Li_7P_3S_{11}$ glass-ceramic electrolyte by dissolution-evaporation method for all-solid-state lithium ion batteries, Electrochim. Acta 219 (2016) 235–240.

[21] N.H.H. Phuc, M. Totani, K. Morikawa, H. Muto, A. Matsuda, Preparation of Li_3PS_4 solid electrolyte using ethyl acetate as synthetic medium, Solid State Ionics 288 (2016) 240–243.
[22] X. Yao, D. Liu, C. Wang, P. Long, G. Peng, Y.-S. Hu, H. Li, L. Chen, X. Xu, High-energy all-solid-state lithium batteries with ultralong cycle life, Nano Lett. 16 (2016) 7148–7154.
[23] S.J. Sedlmaier, S. Indris, C. Dietrich, M. Yavuz, C. Dräger, F. von Seggern, H. Sommer, J. Janek, Li_4PS_4I: a Li^+ superionic conductor synthesized by a solvent-based soft chemistry approach, Chem. Mater. 29 (2017) 1830–1835.
[24] M. Calpa, N.C. Rosero-Navarro, A. Miura, K. Tadanaga, Instantaneous preparation of high lithium-ion conducting sulfide solid electrolyte $Li_7P_3S_{11}$ by a liquid phase process, RSC Adv. 7 (2017) 46499–46504.
[25] N.H.H. Phuc, K. Morikawa, T. Mitsuhiro, H. Muto, A. Matsuda, Synthesis of plate-like Li_3PS_4 solid electrolyte via liquid-phase shaking for all-solid-state lithium batteries, Ionics 23 (2017) 2061–2067.
[26] M. Calpa, N.C. Rosero-Navarro, A. Miura, K. Tadanaga, Preparation of sulfide solid electrolytes in the Li_2S-P_2S_5 system by a liquid phase process, Inorgan. Chem. Front. 5 (2018) 501–508.
[27] H.-D. Lim, X. Yue, X. Xing, V. Petrova, M. Gonzalez, H. Liu, P. Liu, Designing solution chemistries for the low-temperature synthesis of sulfide-based solid electrolytes, J. Mater. Chem. A 6 (2018) 7370–7374.
[28] S. Chida, A. Miura, N.C. Rosero-Navarro, M. Higuchi, N.H.H. Phuc, H. Muto, A. Matsuda, K. Tadanaga, Liquid-phase synthesis of Li_6PS_5Br using ultrasonication and application to cathode composite electrodes in all-solid-state batteries, Ceram. Int. 44 (2017) 742.
[29] S. Yubuchi, M. Uematsu, C. Hotehama, A. Sakuda, A. Hayashi, M. Tatsumisago, An argyrodite sulfide-based superionic conductor synthesized by a liquid-phase technique with tetrahydrofuran and ethanol, J. Mater. Chem. A 7 (2019) 558–566.
[30] L. Zhou, K.-H. Park, X. Sun, F. Lalère, T. Adermann, P. Hartmann, L.F. Nazar, Solvent-engineered design of argyrodite Li_6PS_5X (X = Cl, Br I) solid electrolytes with high ionic conductivity, ACS Energy Lett. 4 (2019) 265–270.
[31] H.-J. Deiseroth, J. Maier, K. Weichert, V. Nickel, S.-T. Kong, C. Reiner, Li_7PS_6 and Li_6PS_5X (X: Cl, Br I): possible three-dimensional diffusion pathways for lithium ions and temperature dependence of the ionic conductivity by impedance measurements, Z. Anorg. Allg. Chem. 637 (2011) 1287–1294.
[32] M. Calpa, N.C. Rosero-Navarro, A. Miura, K. Terai, F. Utsuno, K. Tadanaga, Formation mechanism of thiophosphate anions in the liquid-phase synthesis of sulfide solid electrolytes using polar aprotic solvents, Chem. Mater. 32 (2020) 9627–9632.
[33] R.P. Rao, N. Sharma, V.K. Peterson, S. Adams, Formation and conductivity studies of lithium argyrodite solid electrolytes using in-situ neutron diffraction, Solid State Ionics 230 (2013) 72–76.
[34] R.E. Kroon, Nanoscience and the Scherrer equation versus the 'Scherrer–Gottingen equation', S. Afr. J. Sci. 109 (2013) 2.
[35] H. Wang, Z.D. Hood, Y.N. Xia, C.D. Liang, Fabrication of ultrathin solid electrolyte membranes of β-Li_3PS_4 nanoflakes by evaporation-induced self-assembly for all-solid-state batteries, J. Mater. Chem. A 4 (2016) 8091–8096.
[36] Z.C. Liu, W.J. Fu, E.A. Payzant, X. Yu, Z.L. Wu, N.J. Dudney, J. Kiggans, K.L. Hong, A.J. Rondinone, C.D. Liang, Anomalous high ionic conductivity of nanoporous β-Li_3PS_4, J. Am. Chem. Soc. 135 (2013) 975–978.
[37] M. Calpa, N.C. Rosero-Navarro, A. Miura, R. Jalem, Y. Tateyama, K. Tadanaga, Chemical stability of Li_4PS_4I solid electrolyte against hydrolysis, Appl. Mater. Today 22 (2021) 100918.
[38] M. Calpa, H. Nakajima, S. Mori, Y. Goto, Y. Mizuguchi, C. Moriyoshi, Y. Kuroiwa, N.C. Rosero-Navarro, A. Miura, K. Tadanaga, Formation mechanism of β-Li_3PS_4 through decomposition of complexes, Inorg. Chem. 60 (2021) 6964–6970.
[39] H.J. Deiseroth, S.T. Kong, H. Eckert, J. Vannahme, C. Reiner, T. Zaiß, M. Schlosser, Li_6PS_5X: a class of crystalline Li-rich solids with an unusually high Li^+ mobility, Angew. Chem. Int. Ed. 47 (2008) 755–758.
[40] O. Pecher, S.-T. Kong, T. Goebel, V. Nickel, K. Weichert, C. Reiner, H.-J. Deiseroth, J. Maier, F. Haarmann, D. Zahn, Atomistic characterisation of Li^+ mobility and conductivity in $Li_{7-x}PS_{6-x}I_x$ argyrodites from molecular dynamics simulations solid-state NMR, and impedance spectroscopy, Chem. – A Eur. J. 16 (2010) 8347–8354.
[41] R.P. Rao, S. Adams, Studies of lithium argyrodite solid electrolytes for all-solid-state batteries, Phys. Status Solidi (a) 208 (2011) 1804–1807.
[42] S. Boulineau, M. Courty, J.-M. Tarascon, V. Viallet, Mechanochemical synthesis of Li-argyrodite Li_6PS_5X (X = Cl, Br I) as sulfur-based solid electrolytes for all solid state batteries application, Solid State Ionics 221 (2012) 1–5.
[43] P.R. Rayavarapu, N. Sharma, V.K. Peterson, S. Adams, Variation in structure and Li^+-ion migration in argyrodite-type Li_6PS_5X (X = Cl, Br I) solid electrolytes, J. Solid State Electrochem. 16 (2012) 1807–1813.